Emulsion Stabilization and Flocculation in CO_2. 2. Dynamic Light Scattering

M. Z. Yates, M. L. O'Neill, and K. P. Johnston*

Department of Chemical Engineering, The University of Texas at Austin, Austin, Texas 78712

S. Webber

Department of Chemistry, The University of Texas at Austin, Austin, Texas, 78712

D. A. Canelas, D. E. Betts, and J. M. DeSimone

Department of Chemistry, The University of North Carolina, Chapel Hill, North Carolina, 27599-3290

Received November 18, 1996; Revised Manuscript Received April 21, 1997[⊗]

ABSTRACT: Dynamic light scattering (DLS) was used to investigate steric stabilization and flocculation of dilute poly(2-ethylhexyl acrylate) (PEHA, $M_w = 92$K) emulsions in liquid CO_2 at 25 °C by monitoring changes in droplet size over time at various CO_2 densities. Two steric stabilizers were investigated: a homopolymer, poly(1,1-dihydroperfluorooctyl acrylate) (PFOA, $M_w = 1 \times 10^6$), and a block copolymer, polystyrene ($M_n = 4.5$K g/mol)-*b*-PFOA ($M_n = 25$K). For a concentration of 0.03 wt %, aggregates of PS-*b*-PFOA were observed in CO_2 with an average hydrodynamic diameter of approximately 80 nm and a polydispersity index of 0.2−0.3 from the method of cumulants. Critical flocculation densities (CFDs) of PEHA emulsions were determined by lowering the CO_2 density at constant temperature to induce flocculation. The CFDs of the emulsions agree closely with the Θ point density of PFOA in CO_2 for both the homopolymer and block copolymer stabilizers. Above the CFD, the emulsions have an average droplet size of 400−600 nm and are stable over several hours. With shear, the average droplet size of emulsions stabilized with PS-*b*-PFOA decreases with time because of shear-enhanced flocculation, and subsequent sedimentation of the flocculated droplets. The flocculation of the emulsion is attributed to a depletion mechanism induced by PS-*b*-PFOA aggregates in solution.

Introduction

Liquid or supercritical carbon dioxide is an appealing alternative to many traditional liquid solvents for materials processing, extraction processes, and chemical reactions due to its low cost and environmentally benign nature. However, most nonvolatile hydrophilic and lipophilic compounds have low solubility in CO_2 because of its low polarizability per volume and lack of a permanent dipole. Surfactants can be used to increase solubilization into CO_2 by forming thermodynamically stable water-in-CO_2 microemulsions.[1−4] Furthermore, surfactants with sufficiently long tails can sterically stabilize latexes in carbon dioxide formed by dispersion polymerization[5−7] and by precipitation with a compressed fluid antisolvent.[8,9] However, very few commercially available surfactants are soluble in CO_2,[10,11] and relatively little is known about the design of surfactants for interfaces containing CO_2. In order to develop effective surfactants, it is essential to have a fundamental understanding of surfactant aggregation, phase behavior, and colloidal stabilization and flocculation mechanisms in CO_2.

Materials with low solubility parameters, such as those containing silicon and fluorine, have been found to be highly soluble in CO_2 at moderate temperatures and pressures.[12−15] These substances have been coined "CO_2-philic" because they are chemically dissimilar to both "hydrophilic" and "lipophilic" compounds.[12] Surfactants can be designed with a "CO_2-philic" group, and a "CO_2-phobic" group that may be either hydrophilic or lipophilic in nature. Thus, either hydrophilic or lipophilic materials may be dispersed in a CO_2 continuous phase in the form of microemulsions, emulsions, or latexes.

In order to provide steric stabilization, a surfactant must overcome the attractive van der Waals forces between emulsion droplets in solution. According to Napper, attractive droplet−droplet forces become significant at distances on the order of 5 nm or less for colloidal-sized droplets.[16] An effective stabilizer must have a high enough molar mass to prevent the droplets from approaching closer than this distance. A significant development in the use of surfactants for steric stabilization in CO_2 came with the discovery of polymeric compounds that are highly soluble in CO_2 at moderate conditions.[12,14,17] Poly(1,1-dihydroperfluorooctyl acrylate) (PFOA) is soluble in CO_2 to 5 wt % at moderate pressures (125 bar), even with the molecular weight exceeding 1×10^6.[18] It should be emphasized that the actual backbone length of PFOA is only a small fraction of that of a hydrocarbon surfactant with the same molecular weight due to the high molecular weight of the fluorinated side chain. A recent small angle neutron scattering investigation demonstrated that PFOA has a positive second virial coefficient in CO_2, indicating that CO_2 is a thermodynamically good solvent for this polymer at moderate pressures.[19]

Flocculation can be induced in a sterically stabilized system by reducing the solvating power of the continuous phase for the stabilizing moiety, through changes in temperature or pressure or by addition of an antisolvent. Many experimental studies of sterically stabilized dispersions have shown that there exists a point at which very small changes in the temperature of the continuous phase result in a dramatic change in steric stability. This "critical flocculation temperature" is

[⊗] Abstract published in *Advance ACS Abstracts,* July 15, 1997.

S0024-9297(96)01694-4 CCC: $14.00

strongly related to the Θ point of the stabilizing moiety in free solution.[16] At the Θ point, the stabilizing moieties collapse. The degree of collapse versus temperature is sharp for infinite molecular weight and becomes more gradual as molecular weight decreases. After collapse, steric repulsion becomes much weaker. Flocculation has been induced by either increasing or decreasing temperature. In many cases, critical flocculation temperatures were found to correspond to the Θ temperature for either the upper critical solution temperature (UCST) or the lower critical solution temperature (LCST).[20] The concept of an analogous "critical flocculation density" in compressible solvents has not been explored experimentally.

Dynamic light scattering (DLS) is used commonly to measure hydrodynamic diameters of micelles, emulsions, and latexes from several nanometers up to 1−2 μm, as reviewed thoroughly in the literature.[21−23] It has provided a great deal of information about micelles and microemulsions in supercritical xenon, ethane, and propane.[24−27] Small angle X-ray (SAXS) scattering has been used to discover graft copolymer micelles up to 25 nm in diameter in supercritical CO_2.[28] Dynamic light scattering would be particularly useful for characterizing emulsions in CO_2, which have not been studied previously by scattering techniques.

Our objective is to achieve a fundamental understanding of the mechanisms of emulsion stabilization and flocculation in CO_2 by utilizing *in-situ* measurements. In this study, dynamic light scattering (DLS) is utilized to investigate steric stabilization and flocculation of emulsions, emulsion droplet size, surfactant aggregation, and surfactant phase behavior in CO_2. We chose to study poly(2-ethylhexyl acrylate) (PEHA, $M_w = 9.2 \times 10^4$) as an example of a moderately polar organic liquid dispersed phase that is insoluble in CO_2. Furthermore, it was chosen to emulate poly(methyl methacrylate) latexes formed in CO_2 by dispersion polymerization[6,18] and precipitation with a compressed fluid antisolvent.[8] The stabilizers, PFOA and a polystyrene−PFOA block copolymer (PS-*b*-PFOA), have recently been shown to stabilize polymer latexes produced during dispersion polymerizations in CO_2.[5,18] By forming dispersions with shear rather than by polymerization, the experimental conditions are much more clearly defined, and size measurements can be made in-situ, which is important for examining stabilization and flocculation mechanisms. DLS was used to measure emulsion droplet size and the intensity of scattered light over time to study the mechanisms of flocculation and sedimentation at various densities. Also, the effect of shear in the form of stirring and recirculation through a 100 μm i.d. capillary tube on the stability of the emulsion was examined. To provide a basis for the experiments with emulsions, we first present results of DLS studies of stabilizer phase behavior and of the aggregation of PS-*b*-PFOA in CO_2. The determination of emulsion droplet size is complementary to our companion study[29,30] of turbidimetry and interfacial tension measurements, for the same dispersed phase and surfactants. Together, these three techniques provide a thorough description of the emulsion properties.

Experimental Section

Materials. Poly(2-ethylhexyl acrylate), PEHA ($M_w = 92$K, $M_n = 32$K), was synthesized by Air Products and Chemicals (Allentown, PA) and used as received. The PFOA stabilizer had a molecular weight of approximately 1×10^6. The PS-*b*-PFOA block copolymer had a PS M_n of 4.5×10^3 and a PFOA M_n of 2.5×10^4. The polydispersity index of the PS block was determined by gel permeation chromatography and found to be 1.7. The polydispersity of the PFOA block could not be measured due to its insolubility in common solvents. However, it was estimated that the entire block copolymer has a polydispersity index greater than 2.0. Both stabilizers were synthesized and characterized at the University of North Carolina[5,29,31] and were used as received. Instrument grade carbon dioxide (99.99% purity) was filtered through a 0.5 μm porous metal filter before use.

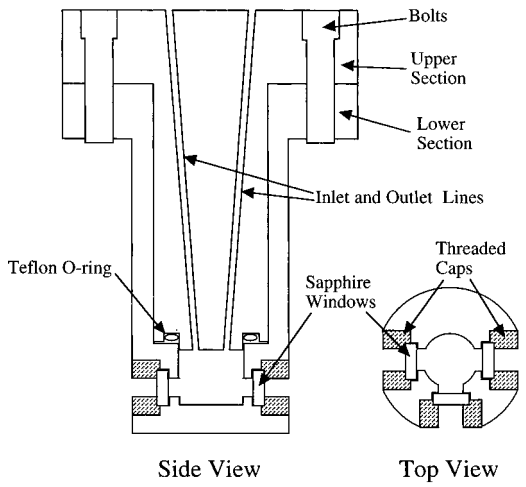

Figure 1. Cross section of the DLS cell.-

DLS Measurements. Dynamic light scattering measurements were made using a Brookhaven model BI-2030 AT digital correlator with 72 real time channels. The incident beam was from a 15 mW helium−neon laser ($\lambda = 632.8$ nm) mounted to a Brookhaven model BI-200 goniometer. A Lauda model RMS-6 recirculator provided temperature control of the scattering cell in the goniometer. All measurements were taken at a scattering angle of 90°.

All of the physical properties of the continuous phase were assumed to be equivalent to that of pure CO_2. The CO_2 density was calculated from Wagner's equation of state.[32] The viscosity was obtained using the correlation proposed by Vesovic.[33] The refractive index was calculated from a virial equation for the molar refractivity of CO_2 at 25 °C.[34] The average droplet size and polydispersity were determined from the autocorrelation function using a second-order method of cumulants analysis.[35]

Apparatus. The stainless steel high-pressure cell for DLS is shown in Figure 1. The 0.82 cm^3 scattering cell consists of two sections that were bolted together using a flange and sealed with a Teflon O-ring. The lower section of the cell contained three sapphire windows at right angles, each 0.635 cm in diameter by 0.229 cm thick. The aperture for each window was approximately 0.3 cm in diameter. The diameter and height of the axial cavity were 1 and 0.95 cm, respectively. The windows were sealed with Teflon O-rings and held in place with threaded stainless steel caps that fit flush to the outer cell body. The lower half of the cell was submerged in a temperature-controlled xylene bath in the goniometer and the upper half of the cell was insulated. Measured sizes obtained from the high-pressure cell were compared with those from a standard glass light scattering cell using an aqueous polystyrene latex standard at ambient pressure. Size measurements were repeated three times for each cell. The mean average diameter measured using a standard glass cell was 506 nm, while the average diameter measured using the high-pressure cell was 520 nm, a satisfactory result.

The complete apparatus for studies of phase behavior and emulsion droplet size is shown in Figure 2. The light scattering cell was connected to a 28 mL magnetically stirred variable-volume view cell that has been described elsewhere.[36] The contents of the view cell were recirculated and filtered through the scattering cell using a Milton/Roy Minipump. A 0.318 cm diameter 0.5 μm porous metal filter (MOTT Metal-

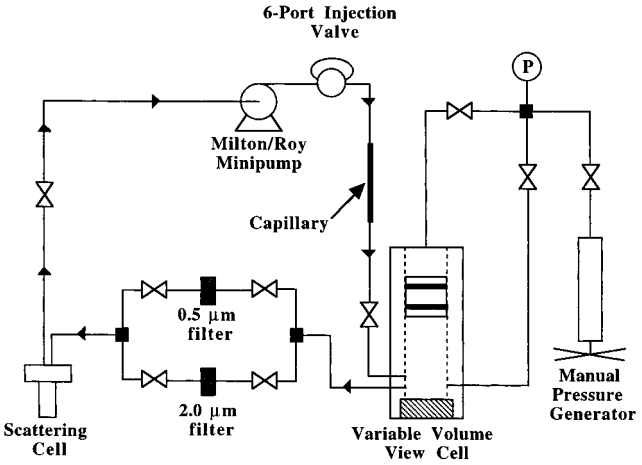

Figure 2. Flow diagram of the DLS/phase behavior apparatus.

lurgical) was used to remove particulates before phase behavior measurements or forming emulsions. A 0.318 cm diameter 2 μm (Valco) filter was used to filter emulsions, as the finer filter would restrict the flow of the emulsion droplets. Two three-way valves were used to switch between the two filters. The dispersed phase was introduced via a 7.1 μL sample loop connected to a six-port rotary valve (Valco). The shear necessary to form the emulsion was obtained by recirculating the heterogeneous mixture through a 5 cm long fused silica capillary with an inner diameter of 100 μm and an outer diameter of 190 μm. The capillary was sheathed in a 5 cm long section of PEEK tubing with a $^1/_{16}$ in. outer diameter and a 0.01 in. inner diameter. The pressure seal was made on the PEEK tubing, and the capillary was held in place by compression of the ends of the PEEK tubing around the capillary. Since a variable volume cell was used, the total volume of the flow system was dependent upon the pressure. At the pressure used for injection and recirculation of the dispersed phase, the volume of the system was 12.3 mL. At the lowest pressure studied, the volume of the system was 13.5 mL. Pressure was controlled with a 100 mL Ruska manual syringe pump and measured to ±0.2 bar with a Sensotec digital pressure gauge.

Procedure. A solution of 0.05 wt % stabilizer/CO_2 was used for both the PFOA and PS-*b*-PFOA emulsion stability studies. The stabilizers were dissolved in CO_2 at 25 °C and 172−207 bar (0.90−0.92 g/mL) while the contents were stirred for at least 8 h. After the stabilizer was dissolved, the solution was recirculated through the 0.5 μm porous metal filter for 10−15 min at a flow rate of 4 mL/min to remove any particulate matter. The phase boundary of the stabilizer was then determined by measuring the average scattered intensity from the light scattering cell as the pressure was lowered in increments. Each intensity measurement was taken after a period greater than 10 min when the temperature and pressure became constant. The pressure was lowered in smaller increments near the phase boundary to reduce the effects of thermal gradients. The point at which the scattered intensity began to increase sharply agreed with the onset of slight visual turbidity in the view cell to within ±2 bar, although the intensity measurements provided a more objective means of assigning a phase boundary. On the basis of visual measurements of phase boundaries before and after filtration, the 0.5 μm filter did not remove a significant fraction of the surfactant because the pressure of the phase boundary remained constant.

After the stabilizer phase boundary was determined, the emulsion was formed by introducing the PEHA into the stabilizer/CO_2 solution at 172.4 bar and 25 °C (0.896 g/mL) through the silica capillary at a flow rate of 4 mL/min. Since a single head piston pump was used, the actual recirculation rate pulsed from approximately 0−8 mL/min. The view cell was stirred during recirculation to obtain a homogeneous mixture throughout. The emulsion was recirculated through a 2 μm filter before entering the light scattering cell. Once a homogeneous mixture was obtained, the visual turbidity of the emulsion did not appear to change during 15 min of recirculation.

Theory

The intensity autocorrelation function is given by

$$G_2(\tau) = \langle I(t)I(t+\tau)\rangle \tag{1}$$

where $I(t)$ is the intensity of scattered light at a given time and τ is a delay time. Provided that the number of particles in the scattering volume is large enough, the intensity autocorrelation function is related to the modulus of the field autocorrelation function $g_1(\tau)$ by[21]

$$G_2(\tau) = A + B[g_1(\tau)]^2 \tag{2}$$

where A and B are instrumental factors.

For a solution of monodisperse spherical particles, $g_1(\tau)$ is given by

$$g_1(\tau) = \exp(-q^2 D\tau) \tag{3}$$

where $q = (4\pi n/\lambda_0)\sin(\theta/2)$, n is the refractive index of the continuous phase, λ_0 is the wavelength of the incident light, θ is the scattering angle, q is the scattering vector, and D is the diffusion coefficient of the droplets in solution. From the diffusion coefficient, the hydrodynamic diameter can then be calculated using the Stokes−Einstein equation:

$$D = \frac{kT}{3\pi\eta d} \tag{4}$$

where k is Boltzmann's constant, T is the temperature, η is the viscosity of the continuous phase, and d is the hydrodynamic diameter of the particle.

For a solution of polydisperse spherical particles, the method is essentially the same except that eq 3 above is no longer a single exponential function but is multiexponential. The cumulants method is employed to obtain an average droplet size and polydispersity index from $g_1(\tau)$.[35] In this method, the natural log of $g_1(\tau)$ versus τ is fitted to a second-order polynomial. The coefficient of the first-order term is an average decay rate, $q^2\bar{D}$, where $\bar{D}$ is the average diffusion coefficient. Equation 4 is used to calculate an average droplet size from $\bar{D}$. The coefficient of the second-order term is defined as a polydispersity index, which goes to zero for a monodisperse solution.

Dynamic light scattering requires low concentrations of the dispersed phase so that the effects of multiple scattering and droplet−droplet interactions on the measured droplet size can be avoided. The upper concentration limit is dependent upon the scattering path length and the ratio of refractive index of the dispersed phase and continuous phase. Typically, multiple scattering effects will begin to occur when the volume fraction of the dispersed phase is above 10^{-3}−10^{-4}.[21] Multiple scattering will cause the intensity autocorrelation function $G_2(\tau)$ to decay at a faster rate, and the size measured by DLS will then be smaller than the actual size. Multiple scattering will also cause the laser beam to spread out into a "halo"; this behavior was not observed at the concentrations used in this study. Other reasons that suggest multiple scattering was negligible are that the emulsions were only slightly

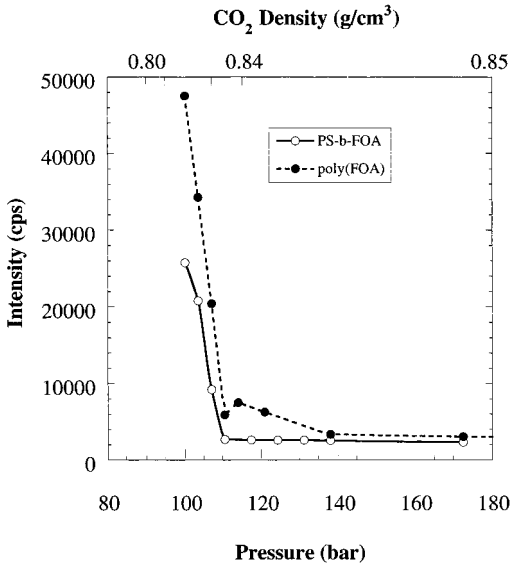

Figure 3. Phase boundary of 0.03 wt % PFOA and 0.03 wt % PS-*b*-PFOA at 25 °C from average scattered intensity.

turbid in appearance and the dispersed phase concentration was only 0.04 wt %.

Results

Phase Behavior. The phase boundary for 0.03 wt % PFOA in CO_2 determined by the average scattered intensity is shown in Figure 3 at 25 °C. The intensity increases modestly at approximately 120 bar and then increases sharply at 110 bar. The phase boundary or cloud point was assigned as 110 bar. Since the PFOA sample is somewhat polydisperse, the slight increase in scattered intensity observed at 120 bar is likely due to the precipitation of a small fraction of higher molecular weight material. Recently, the phase behavior of PFOA of the same molecular weight was measured visually over a wide range of concentrations and temperatures in CO_2.[18] This system exhibits lower critical solution temperature type phase behavior. None of these previous measurements were carried out below 30 °C or at concentrations lower than 0.09 wt %. However, our new results at 0.03 wt % and 25 °C agree with trends in the earlier measurements extrapolated to lower concentrations and temperatures.

The phase behavior of 0.03 wt % PS-*b*-PFOA at 25 °C is also shown in Figure 3. The sharp increase in scattered intensity below 110 bar indicates a cloud point. The sharper phase boundary for this block copolymer versus PFOA may indicate a lower polydispersity for this sample. At a concentration of 0.03 wt %, the cloud points of PFOA and PS-*b*-PFOA are the same. This is strictly coincidental, since the lower molecular weight PS-*b*-PFOA will cause the phase boundary to shift to a lower pressure, while the addition of the CO_2-insoluble polystyrene block will shift the phase boundary to a higher pressure.

A phase behavior test was done to determine if a fraction of PEHA was soluble in CO_2. PEHA was added to attempt to form a solution of 0.009 wt % at 25 °C and 345 bar, but very little dissolved. When the pressure was reduced to 83 bar, the CO_2 phase became slightly opaque, indicating that a very small amount of PEHA had dissolved at 345 bar. This small amount of solubilized PEHA did not give any signal in DLS experiments for a constant pressure of 172 bar.

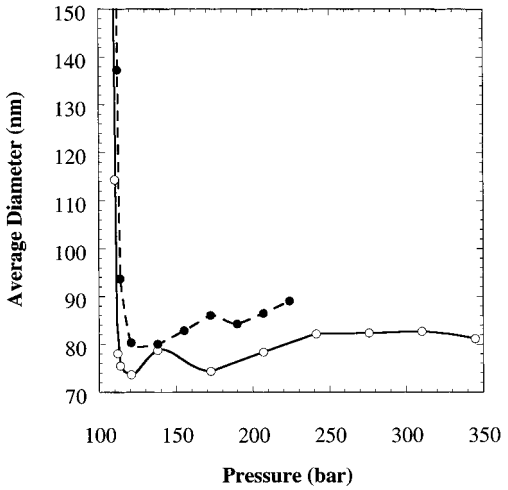

Figure 4. Average hydrodynamic diameter of PS-*b*-PFOA aggregates at 0.03 wt % and 25 °C showing two different experiments at the same conditions.

PS-*b*-PFOA Aggregate Formation. Block copolymers of polystyrene and PFOA have been shown to form aggregates in CO_2, as determined by small angle neutron scattering.[30,37] Aggregates of fluorinated surfactants generally are not amenable to study with light scattering due to the low difference in refractive index between most fluorinated compounds and CO_2.[38,39] We found that an autocorrelation function was not discernible for PFOA/CO_2 solutions above the phase boundary, indicating that the 0.5 μm filter removed dust successfully. The optical contrast was too low since the refractive index of PFOA is 1.34 and that of CO_2 is approximately 1.20−1.24 at these conditions. It may be possible to determine solution properties of PFOA in CO_2 using light scattering at smaller angles where the scattered intensity is higher. However, measurements were limited to 90° due to the geometry of the high-pressure scattering cell. For PS-*b*-PFOA solutions at 25 °C, the autocorrelation function was well above the baseline at all pressures above the cloud point. Inversion of the autocorrelation function indicated the presence of large aggregates in solution. These aggregates are observable because of their large size as well as the improved optical contrast between CO_2 and stabilizer due to the addition of the polystyrene block ($n_d = 1.59$).

Figure 4 gives the average hydrodynamic diameter calculated from the correlation function versus pressure for the PS-*b*-PFOA solution at 25 °C for two experiments at the same conditions. At the higher pressures in the one-phase region, the measured diameters range from approximately 75 to 90 nm, and the polydispersity index calculated from the method of cumulants analysis was 0.2−0.3. The average diameter obtained by DLS is heavily weighted by larger aggregates. Given this fact along with the high polydispersity of the aggregates, a significant amount of the distribution is likely due to smaller micelle-like aggregates.

The rather large PS-*b*-PFOA aggregates were likely due to the polydispersity in each of the copolymer blocks. The ratio of PFOA to PS must be some minimum value for the copolymer to dissolve in CO_2 at a given temperature and pressure. A fraction of the copolymer may have a lower PFOA to PS ratio and thus remain insoluble at the conditions studied. This hypothesis was supported by further phase equilibria measurements. The PS-*b*-PFOA solution was clear in appearance at the

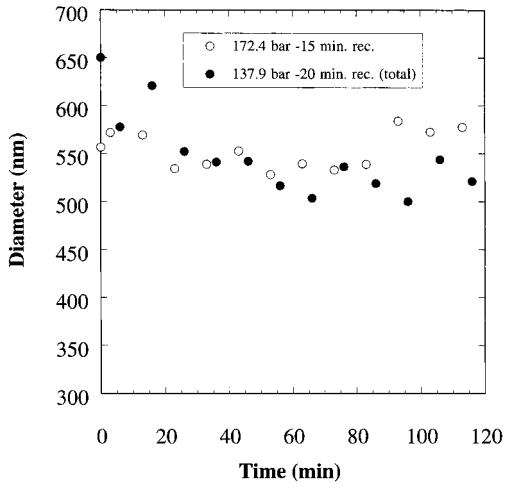

Figure 5. Stability of 0.04 wt % PEHA emulsion with 0.03 wt % PFOA stabilizer at pressures well above the stabilizer phase boundary.

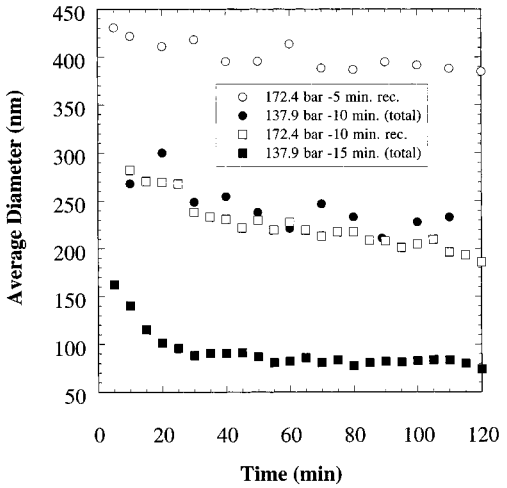

Figure 6. Effect of recirculation time (shear) on the average droplet size for 0.04 wt % PEHA emulsion with 0.03 wt % PS-*b*-PFOA stabilizer at 25 °C and pressures well above the stabilizer phase boundary.

concentration studied by DLS (0.03 wt %). At 0.1 wt %, the PS-*b*-PFOA solution had a slight orange tint, indicative of Rayleigh scattering, at 345 bar and 25 °C. At 0.35 wt %, the PS-*b*-PFOA solution was slightly turbid in appearance at the same conditions. Therefore, it is likely that a small fraction of the 0.03 wt % solution was not fully soluble at the conditions studied. Single chains or even micelles can adsorb to this dispersed fraction, producing large aggregates. This behavior may be analogous to the very large particles observed by light scattering for poly(propylene oxide)−poly(ethylene oxide)−poly(propylene oxide) (Pluronic L64) solutions near the critical micelle temperature.[40] This triblock copolymer with a molecular weight of approximately 2900 is composed of approximately 40% ethylene oxide by weight. In this study, the insoluble fraction of Pluronic L64 was removed by filtration of the large particles and the anomalous behavior was no longer seen.

Emulsion Stability at High CO_2 Densities. The PEHA was injected at 25 °C and 241.4 bar without stabilizer. Initially, the PEHA was dispersed into the view cell, forming a slightly turbid emulsion. However, the resulting emulsion was very unstable. After recirculating for 5 min, the PEHA had completely settled from the CO_2. Very weak scattering was measured from the DLS cell after recirculation. The approximate size appeared to be >2 μm.

To study the effect of a stabilizer, PEHA was injected into PFOA in CO_2 solution at 172.4 bar and 25 °C. For this emulsion, the initial recirculation (shear) time before taking measurements was 15 min. At the recirculation rate used, this time corresponds to recirculation of 5 residence volumes, which should be sufficient to form a homogeneous mixture. The resulting emulsion was slightly turbid in appearance. The average droplet size was measured repeatedly at the same conditions over a 2 h period, as shown in Figure 5. The reproducibility of the particle size formed was approximately ±50 nm. The emulsion was then recirculated for an additional 5 min to shear the solution. Recirculation was then stopped, and the pressure was reduced to 137.9 bar. Repeated size measurements were then taken at 137.9 bar and 25 °C for an additional 2 h period. The droplet sizes ranged between 500 and 650 nm with an average polydispersity index of 0.3 from the method of cumulants analysis. The average droplet size changed very little throughout the experiment, indicating good steric stabilization. Little, if any, flocculation occurred at either pressure.

For the emulsions stabilized with PS-*b*-PFOA, it was found that the droplet size was very dependent upon the emulsification conditions. The average droplet size obtained was reproducible to approximately ±50 nm. Figure 6 shows the results of two experiments in which the recirculation (shear) time was varied. In one experiment, the initial emulsion was recirculated for 5 min before taking measurements at 172.4 bar for 2 h (open circles), followed by 5 min of additional recirculation and depressurization to 137.9 bar (filled circles). In the second experiment, the initial recirculation time was 10 min (open squares), with 5 min of additional recirculation before the readings at 137.9 bar (filled squares). Unlike the case for the emulsion stabilized with PFOA, increased recirculation of the PS-*b*-PFOA stabilized emulsion results in an appreciable decrease in average droplet size. Visual observations in the view cell also indicated that an increase in the recirculation time results in clarification of the emulsion with a small pool of PEHA forming at the bottom of the view cell.

Turbidity measurements were carried out to further investigate the effect of shear on the emulsion in the presence of PS-*b*-PFOA (Figure 7), by following a procedure described elsewhere.[29] The apparatus was identical to the DLS apparatus except the 90° scattering cell was replaced with a transmission cell of 1.0 cm path length. Turbidity measurements were carried out at 633 nm using the same PS-*b*-PFOA and PEHA concentrations used in the DLS measurements. The PEHA was injected at 172.4 bar and 25 °C and recirculated for 5 min prior to taking measurements. Repeated measurements of emulsion turbidity were taken for 15 min; then the emulsion was recirculated for an additional 5 min. This procedure was repeated four times. The turbidity of the emulsion dropped dramatically during each recirculation period. Since the measured droplet size decreases along with the turbidity, it is unclear weather the reduction in turbidity is due primarily to the lower scattered intensity of smaller particles or to the presence of a smaller dispersed phase volume fraction due to flocculation and sedimentation. However, visual observations of the formation of a small pool of PEHA bulk phase at the bottom of the variable volume view cell indicate that at least some of the

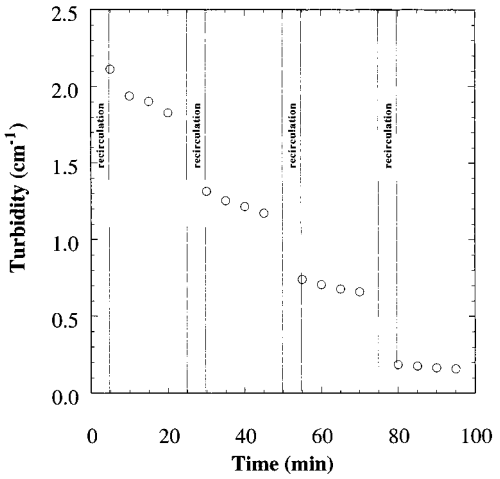

Figure 7. Effect of recirculation time (shear) on the emulsion turbidity at 633 nm for 0.04 wt % PEHA emulsion with 0.03 wt % PS-*b*-PFOA stabilizer at 25 °C. Recirculation rate of 4 mL/min.

reduction in turbidity is due to sedimentation and coalescence of flocculated emulsion droplets.

Several factors may potentially contribute to the reduction in acrylate particle size with shear for the PS-*b*-PFOA stabilized system. (1) The mixing of CO_2-soluble surfactant with the injected dispersed phase increases with recirculation, leading to a reduction in the interfacial tension, such that smaller and smaller droplets are produced by shear. The smaller droplets scatter less light and would reduce the turbidity. (2) Greater mixing time of acrylate droplets with the surfactant solution can convert emulsion droplets to transparent microemulsion droplets. (3) Microemulsion droplets or surfactant aggregates may destabilize the emulsions through a depletion mechanism, which is accelerated by shear. (4) Shear degrades the stabilizer or dispersed phase. However, shear degradation appears to be negligible on the basis of the lack of any change in emulsion turbidity or stability for cumulative shear times of up to 2 h.[29]

The first factor may be shown to play a small role. The interfacial tension between CO_2 and PEHA is 0.55 dyne/cm at 45 °C and 310 bar.[29] This interfacial tension is sufficiently low to allow PEHA emulsion droplets to be formed in CO_2 without a surfactant, but the droplets flocculate from collisions due to Brownian motion if not protected sterically.[29,30] When the PEHA is initially injected through the capillary, there is little time for the surfactant to adsorb to the interface before droplet breakup occurs. However, after just 5 min of recirculation, the emulsion droplet size is stable without recirculation over a 2 h period. On the basis of a companion study of acrylate emulsions in CO_2, the emulsion droplets would have settled rapidly if they were not stabilized by surfactant.[29,30] Also, the growth of precipitated acrylate on the bottom of the view cell with further recirculation suggests that emulsification due to recirculation was diminishing, not increasing.

To evaluate the importance of the second factor in the reduction of emulsion turbidity, the solubilization of PEHA into PS-*b*-PFOA micelles was measured. The procedure has been described previously.[2] To prevent emulsion formation, the mixture was stirred gently. Experiments were done using the same PS-*b*-PFOA to PEHA ratio as in the DLS experiments (3:4 by weight). It was not possible to dissolve 0.04 wt % PEHA with 0.03 wt % PS-*b*-PFOA at 25 °C at pressures up to 379 bar. Additional experiments were done at a higher PS-*b*-PFOA to PEHA ratio (50:3 by weight) using a slightly different molecular weight PS-*b*-PFOA (PS $M_w = 3.7$K, PFOA $M_w = 27$K). From these experiments, 0.50 wt % PS-*b*-PFOA was unable to significantly solubilize 0.03 wt % PEHA at 25 °C at pressures up to 380 bar. These findings indicate that very little of the PEHA is solubilized and the formation of a transparent microemulsion is not a major factor in the reduction of emulsion turbidity.

The PEHA emulsions studied with DLS had a weight ratio of stabilizer to dispersed phase higher than is normally used for steric stabilization.[16] In our companion study, it was shown that a ratio of PS-*b*-PFOA to PEHA of 0.03 could successfully stabilize an emulsion.[29] The PS-PFOA to PEHA ratio used in DLS measurements was 0.75. The excess surfactant not adsorbed to the PEHA emulsion droplets can exist as unimers and aggregates in the continuous phase. The concentration required for PS-*b*-PFOA to aggregate may be estimated from the discontinuity in the PS/CO_2 interfacial tension with PS-*b*-PFOA concentration for a slightly different molecular weight block copolymer (PS $M_w = 3.7$K, PFOA $M_w = 27$K).[41] The concentration of PS-*b*-PFOA used for the PEHA emulsions is at least 1 order of magnitude higher than that required for aggregate formation. The molecular weight of the copolymer used for the DLS study had a slightly higher polystyrene to PFOA ratio, and as a result, should begin to aggregate at even lower concentrations. Surfactant aggregation is clearly evident in CO_2, as was shown in Figure 4. Thus for 0.03 wt % surfactant, aggregates should continue to exist in the continuous phase even after a portion of the surfactant adsorbs to the PEHA interface.

Previous studies have demonstrated that excess micellized or microemulsified surfactant can act to destabilize emulsion droplets through a depletion mechanism.[42] Upon the close approach of two emulsion droplets, the aggregates are excluded from the region between the two emulsion droplets. This results in an osmotic pressure difference that forces the two droplets together. The shear and turbulent flow produced during recirculation increase the rate of depletion flocculation by increasing the number of collisions between emulsion droplets. From Figure 6, the average droplet size after a total of 15 min of recirculation approaches the measured size of the surfactant aggregates shown in Figure 4. This suggests that the PEHA is largely de-emulsified due to sedimentation of large flocculated droplets, leaving the surfactant aggregates in solution. This mechanism is supported by the presence of a PEHA phase at the bottom of the view cell. On the basis of all of the evidence, shear-enhanced depletion flocculation of emulsion droplets by surfactant aggregates appears to be the most likely cause of the decrease in droplet size.

Critical Flocculation Density Determination. A critical flocculation density for the emulsion was determined by examining the effect of decreasing CO_2 density on the average droplet size. This approach is complementary to a companion study of PEHA emulsion stability using turbidity measurements.[29] Once again, the emulsion was formed at 172.4 bar and 25 °C using a recirculation time of 15 min. Size measurements were taken without any additional recirculation, and the

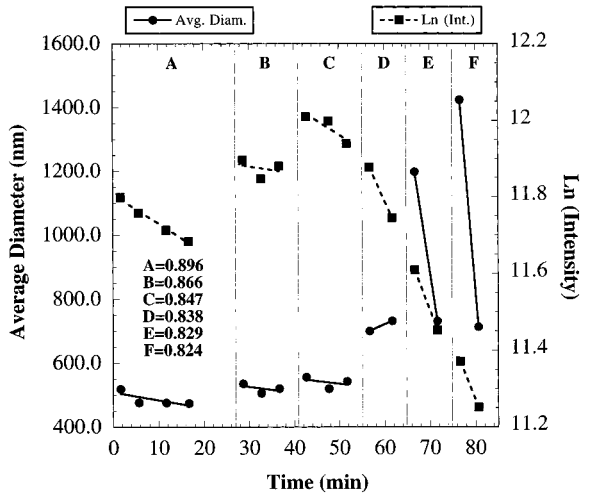

Figure 8. Critical flocculation density of 0.04 wt % PEHA emulsion stabilized with 0.03 wt % PFOA. CO_2 densities in regions A through F are given in g/mL.

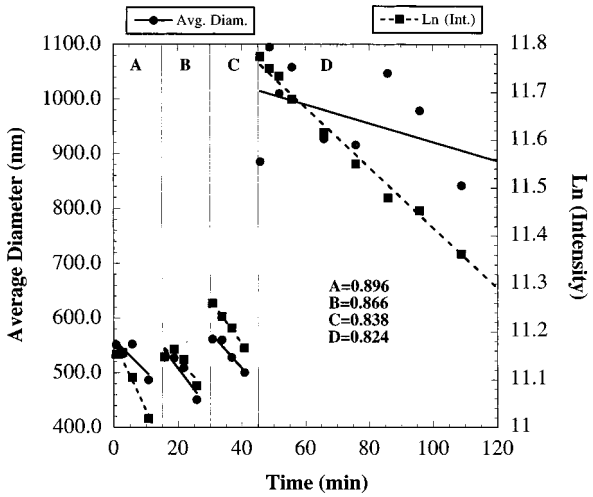

Figure 9. Critical flocculation density of 0.04 wt % PEHA emulsion stabilized with 0.03 wt % PS-*b*-PFOA. CO_2 densities in regions A through D are given in g/mL.

pressure was lowered in increments. The sizes of the increments were decreased as the phase boundary of the stabilizer was approached. Figure 8 shows the results for the PFOA-stabilized emulsion. Average size and intensity measurements are plotted versus time for the various CO_2 densities, since density is a better measure of the solvating power of CO_2 than pressure. At densities well above the phase boundary for PFOA (>0.847 g/mL), the average droplet size changes little with time. When the density is reduced from 0.847 to 0.838 g/mL, the average droplet size increases from 543 to 700 nm. As the CO_2 density was further lowered to 0.829 g/mL, the average droplet size increased rapidly to 1200 nm. A repeated measurement at the same density 5 min later indicated that the average size had decreased to 730 nm. The immediate increase in average droplet size later followed by a reduction in average droplet size is indicative of simultaneous flocculation and sedimentation of the emulsion.[43] The initial increase in the average droplet size is due to the formation of droplet aggregates during flocculation. The larger flocs then settle from the scattering volume faster than smaller ones, reducing the average droplet size. Additional flocculation and sedimentation were observed as the CO_2 density was lowered further to 0.824 g/mL.

The increase in droplet size between 0.847 and 0.838 g/mL indicates the onset of flocculation. This CFD agrees very closely with the value of 0.84 g/mL for the same system at higher concentrations determined from turbidity measurements.[29] The correlation of Θ point density with the CFD is not as well-defined theoretically for homopolymer stabilization as it is for adsorbed block copolymers. However, the CFD corresponds closely to the cloud point density of PFOA shown in Figure 3. The cloud point density (0.834 g/mL) should be close to the Θ point density for PFOA at 25 °C, because the molar mass of PFOA is extremely high, approaching infinity.[29]

Sedimentation of the flocs can also be observed by decreases in the average scattered intensity of the emulsion, also shown in Figure 8. The intensity changes little with time above the CFD. Below the CFD, however, the scattered intensity decreases continuously. Visual observations of the emulsion through the view cell indicated that the emulsion became clear after 20 min at 0.009−0.014 g/mL below the phase boundary, and a small pool of PEHA was observed at the bottom of the view cell.

Figure 9 shows the results for the PEHA emulsion stabilized by PS-*b*-PFOA. Due to the instability of the emulsion with recirculation, this emulsion was formed at 172.4 bar and 25 °C with only 5 min of recirculation. As for emulsions with PFOA, the average size of the emulsion droplets remains relatively constant at approximately 525 nm at CO_2 densities well above the stabilizer phase boundary (>0.838 g/mL). When the density is lowered from 0.838 to 0.824 g/mL, a sharp increase in average droplet size to 1100 nm is observed. Thus, the CFD for this system also corresponds almost exactly to the Θ point density of the stabilizing block, PFOA, in CO_2.

The behavior of the emulsion stabilized with PS-*b*-PFOA below the CFD is markedly different than that of the PFOA-stabilized emulsion. The flocculated droplet sizes did not become quite as large as with PFOA-stabilized emulsions. Also, the decay in droplet size due to sedimentation of the emulsion droplets was much slower for the PS-*b*-PFOA-stabilized emulsion below the CFD. The PS-*b*-PFOA-stabilized emulsion droplets reached an average diameter of 1100 nm below the CFD, and after 1 h, the diameter fell to approximately 850 nm. In contrast, the average droplet size of the PFOA-stabilized emulsion increased rapidly to 1200 nm below the CFD but fell to 700 nm within 5 min due to sedimentation. As discussed by O'Neill et al.[29] the PFOA homopolymer has a very high molecular weight and can adsorb to more than one emulsion droplet below the phase boundary. This bridging flocculation can enhance the rate of flocculation and cause the differences seen for the two different stabilizers below the CFD.

Conclusions

The critical flocculation density (CFD) of sterically stabilized PEHA emulsions has been determined by measuring changes in droplet size and scattered intensity with decreasing CO_2 density. The results are in good agreement with a companion study in which critical flocculation densities of the same systems were determined by turbidimetry.[29] For emulsions stabilized with PFOA homopolymer as well as those stabilized with the block copolymer PS-*b*-PFOA, the CFD is very near the Θ point of the stabilizing moiety in CO_2. Just

below the CFD, emulsions stabilized with PFOA exhibit a sharp increase in average droplet size, followed by a sharp decrease, indicating flocculation and subsequent sedimentation.[43] Emulsions stabilized with PS-*b*-PFOA exhibit a slower flocculation rate below the CFD, due to greater surfactant adsorption and the absence of bridging flocculation.[29] The PS-*b*-PFOA-stabilized emulsion clarified when the emulsion was sheared through recirculation and stirring, as indicated by DLS and turbidimetry. The reduction in turbidity is due to depletion flocculation induced by PS-*b*-PFOA aggregates in solution and subsequent sedimentation of the flocculated droplets. Large PS-*b*-PFOA block copolymer aggregates are observed in solution, which may be due to a dispersed insoluble MW fraction of the block copolymer.

Acknowledgment. We acknowledge support from the Separations Research Program at the University of Texas, the National Science Foundation, and Air Products and Chemicals. Mark O'Neill acknowledges support from the Natural Sciences and Engineering Research Council of Canada. We would also like to acknowledge MOTT Metallurgical Corp. for donation of porous metal filters.

References and Notes

(1) Johnston, K. P.; Harrison, K. L.; Clarke, M. J.; Howdle, S. M.; Heitz, M. P.; Bright, F. V.; Carlier, C.; Randolph, T. W. *Science* **1996**, *271*, 624−626.
(2) Harrison, K.; Goveas, J.; Johnston, K. P. *Langmuir* **1994**, *10*, 3536−3541.
(3) McFann, G. J.; Johnston, K. P. In *Microemulsions: Fundamentals and Applied Aspects*; Kumar, P., Mittal, K. L., Ed.; Marcel Dekker: New York (in press).
(4) Bartscherer, K. A.; Renon, H.; Minier, M. *Fluid Phase Equilib.* **1995**, *107*, 93−150.
(5) Canelas, D. A.; Betts, D. E.; DeSimone, J. M. *Macromolecules* **1996**, *29*, 2818.
(6) DeSimone, J. M.; Maury, E. E.; Menceloglu, Y. Z.; McClain, J. B.; Romack, T. J.; Combes, J. R. *Science* **1994**, *265*, 356.
(7) Yazdi, A. V.; Lepilleur, C.; Singley, E. J.; Lui, W.; Adamsky, F. A.; Enick, R. M.; Beckman, E. J. *Fluid Phase Equilib.* **1996**, *117*, 297−303.
(8) Mawson, S.; Johnston, K. P.; Betts, D. E.; McClain, J. B.; DeSimone, J. M. *Macromolecules* **1997**, *30*, 71.
(9) Mawson, S.; Yates, M. Z.; O'Neill, M. L.; Johnston, K. P. *Langmuir* **1997**, *13*, 1519.
(10) Consani, K. A.; Smith, R. D. *J. Supercrit. Fluids* **1990**, *3*, 51−65.
(11) McFann, G. J. Ph.D. Thesis, The University of Texas, 1993.
(12) DeSimone, J. M.; Guan, Z.; Elsbernd, C. S. *Science* **1992**, *257*, 945.
(13) Hoefling, T. A.; Beitle, R. R.; Enick, R. M.; Beckman, E. J. *Fluid Phase Equilib.* **1993**, *83*, 203−212.
(14) Hoefling, T.; Stofesky, D.; Reid, M.; Beckman, E. J.; Enick, R. M. *J. Supercrit. Fluids* **1992**, *5*, 237−241.
(15) McHugh, M.; Krukonis, V. *Supercritical Fluid Extraction: Principles and Practice*, 1st ed.; Butterworth: Boston, 1986.
(16) Napper, D. H. *Polymeric Stabilization of Colloidal Dispersions*; Academic Press Inc.: New York, 1983.
(17) Newman, D. A.; Hoefling, T. A.; Beitle, R. R.; Beckman, E. J.; Enick, R. M. *J. Supercrit. Fluids* **1993**, *6*, 205−210.
(18) Hsiao, Y.-L.; Maury, E. E.; DeSimone, J. M.; Mawson, S.; Johnston, K. P. *Macromolecules* **1995**, *28*, 8159−8166.
(19) McClain, J. B.; Londono, D.; Combes, J. R.; Romack, T. J.; Canelas, D. A.; Betts, D. E.; Wignall, G. D.; Samulski, E. T.; DeSimone, J. M. *J. Am. Chem. Soc.* **1996**, *118*, 917−918.
(20) Everett, D. H.; Stageman, J. F. *Faraday Discuss. Chem. Soc.* **1978**, *65*, 230−241.
(21) Finsy, R. *Adv. Colloid Interface Sci.* **1994**, *52*, 79−143.
(22) Chu, B. *Laser Light Scattering: Basic Principles and Practice*, 2nd ed.; Academic Press: Boston, 1991.
(23) Pecora, R. *Dynamic Light Scattering: Applications of Photon Correlation Spectroscopy*; Plenum Press: New York, 1985.
(24) Smith, R. D.; Fulton, J. L.; Blitz, J. P.; Tingey, J. M. *J. Phys. Chem.* **1990**, *94*, 781−787.
(25) Fulton, J. L.; Blitz, J. P.; Tingey, J. M.; Smith, R. D. *J. Phys. Chem.* **1989**, *93*, 4198−4204.
(26) Fulton, J. L.; Smith, R. D. *J. Phys. Chem.* **1988**, *92*, 2903−2907.
(27) Blitz, J. P.; Fulton, J. L.; Smith, R. D. *J. Phys. Chem.* **1988**, *92*, 2707−2710.
(28) Fulton, J. L.; Pfund, D. M.; McClain, J. B.; Romack, T. J.; Maury, E. E.; Combes, J. R.; Samulski, E. T.; DeSimone, J. M.; Capel, M. *Langmuir* **1995**, *11*, 4241−4249.
(29) O'Neill, M. L.; Yates, M. Z.; Johnston, K. P.; Wilkinson, S. P.; Canelas, D. A.; Betts, D. E.; DeSimone, J. M. *Macromolecules* **1997**, *30*, 5050−5059 (preceding article in this issue).
(30) O'Neill, M. L.; Yates, M. Z.; Johnston, K. P.; Wilkinson, S. P.; DeSimone, J. M. *Polym. Mater. Sci. Eng.* **1996**, *74*, 228−229.
(31) Guan, Z.; DeSimone, J. M. *Abstracts of Papers*, 206th National Meeting of the *American Chemical Society*, Chicago, Illinois, Fall 1993; American Chemical Society: Washington, DC, 1993; pp 614−615.
(32) Ely, J. F. *CO_2PAC A Computer Program to Calculate the Physical Properties of Pure CO_2*; National Bureau of Standards: Boulder, 1986.
(33) Vesovic, V.; Wakeham, W. A.; Olchowy, G. A.; Sengers, J. V.; Watson, J. T. R.; Millat, J. *J. Chem. Ref. Data* **1990**, *19*, 763−808.
(34) Burns, R. C.; Graham, C.; Weller, A. R. M. *Mol. Phys.* **1986**, *59*, 41.
(35) Koppel, D. E. *J. Chem. Phys.* **1972**, *57*, 4814.
(36) Lemert, R. M.; Fuller, R. A.; Johnston, K. P. *J. Phys. Chem.* **1990**, *94*, 6021−6028.
(37) McClain, J. B.; Betts, D. E.; Samulski, E. T.; DeSimone, J. M. *AIChE 1995 Annual Meeting*, Miami Beach, FL, 1995; AIChE: New York, 1995.
(38) Cotts, P. M. *Macromolecules* **1994**, *27*, 6487−6491.
(39) Kissa, E. *Fluorinated Surfactants: Synthesis, Properties, Applications*; Marcel Dekker: New York, 1994.
(40) Zhou, Z.; Chu, B. *Macromolecules* **1988**, *21*, 2548−2554.
(41) Harrison, K. L.; Rocha, S. R. P. d.; Yates, M. Z.; Johnston, K. P.; Canelas, D.; DeSimone, J. M. Manuscript in preparation.
(42) Binks, B. P.; Fletcher, P. D. I.; Horsup, D. I. *Colloid Surf.* **1991**, *61*, 291−315.
(43) Reddy, S. R.; Melik, D. H.; Fogler, H. S. *J. Colloid Interface Sci.* **1981**, *82*, 116−127.

MA961694S